Sādhanā, Vol. 18, Parts 3 & 4, August 1993, pp. 405–430. © Printed in India.

Boltzmann schemes for continuum gas dynamics

S M DESHPANDE

Computational Fluid Dynamics Laboratory, Department of Aerospace Engineering, Indian Institute of Science, Bangalore 560012, India

Abstract. Many problems arising in the aerodynamic design of aerospace vehicles require the numerical solution of the Euler equations of gas dynamics. These are nonlinear partial differential equations admitting weak solutions such as shock waves and constructing robust numerical schemes for these equations is a challenging task. A new line of research called Boltzmann or kinetic schemes discussed in the present paper exploits the connection between the Boltzmann equation of the kinetic theory of gases and the Euler equations for inviscid compressible flows. Because of this connection, a suitable moment of a numerical scheme for the Boltzmann equation yields a numerical scheme for the Euler equations. This idea called the "moment method strategy" turns out to be an extremely rich methodology for developing robust numerical schemes for the Euler equations. The richness is demonstrated by developing a variety of kinetic schemes such as kinetic numerical method, kinetic flux vector splitting method, thermal velocity based splitting, multidirectional upwind method and least squares weak upwind scheme.

A 3-D time-marching Euler code called BHEEMA based on the kinetic flux vector splitting method and its variants involving equilibrium chemistry have been developed for computing hypersonic reentry flows. The results obtained from the code BHEEMA demonstrate the robustness and the utility of the kinetic flux vector splitting method as a design tool in aerodynamics.

Keywords. Boltzmann equation; kinetic schemes for Euler equation; gas dynamics; computational fluid dynamics; robust numerical schemes.

1. Introduction

Many problems arising in the aerodynamic design of aerospace vehicles require the numerical solution of the Euler equations of gas dynamics. Some notable examples are flow past delta wings, flow through ramjet type intakes of missiles, external supersonic flow around launch vehicles and missiles, and hypersonic re-entry flow. Generally any flow which is nearly attached (that is, not involving separation of the thin viscous layer from the body surface) needs the solution of the Euler equations of motion. These equations also need to be solved in cases of flow problems where viscous effects are approximately taken into account by solving the famous boundary layer equations which again require the inviscid solution. Such problems involve weak viscid-inviscid coupling. Therefore, constructing numerical schemes for solving these equations has been one of the principal subjects of research among the CFD community for the last decade. The Euler equations are nonlinear vector conservation equations and, further, are hyperbolic. These equations are known to admit shocks, which are known as weak solutions from the mathematical point of view. At the Euler level, shocks are gas dynamic discontinuities across which the physical variables density, pressure and temperature, undergo sudden jumps. The challenge in constructing numerical schemes for solving the Euler equations then lies in correctly and accurately computing the weak solutions within the framework of the inviscid approximation. It is therefore highly desirable from the point of view of accuracy and robustness to design numerical schemes which are conservative and upwind, that is, which respect hyperbolicity.

Before the advent of the Boltzmann or kinetic schemes, upwinding has been enforced via flux-vector splitting (see, for example, Van Leer 1982) or via flux-difference splitting (Roe 1981). In the former approach, the flux-vector G is split into two flux-vectors G^+ and G^-, so that the flux-Jacobians (the Jacobians of G^+ and G^- with respect to the conserved vector U) have all-positive and all-negative eigenvalues. In the flux-difference splitting approach, the domain is divided into cells in each of which the state is assumed constant. The fluid variables will, in general, be discontinuous across the cell interfaces. Local 1-D Riemann problems are then solved exactly or approximately and the solutions of these are used to obtain the numerical solution of the Euler equations. Both these approaches have to grapple with the nonlinearity of the Euler equations. The third line of approach employed in constructing conservative upwind schemes is based on what Deshpande (1986c) calls the moment method strategy which is based on the fact that the Euler equations are suitable moments of the Boltzmann equation of the kinetic theory of gases. In some sense, the Boltzmann equation is more fundamental than the Navier–Stokes equations of fluid dynamics because the latter follow from the former when the mean free path of the molecules is much smaller than the characteristic length of the body. In this case, the velocity distribution function is the well-known Chapman–Enskog distribution. The Chapman–Enskog theory is intimately connected with the Navier–Stokes equations. If, on the other hand, the velocity distribution is taken as the Maxwellian distribution, then the suitable moments of the Boltzmann equation yield the Euler equations. Several other workers have also exploited this connection between the Boltzmann and the Euler equations for constructing the Boltzmann schemes (see Pullin 1980, Rietz 1981, Elizarova & Chetverushkin 1985, Kaniel 1988, Perthame 1990, Croisille & Delorme 1991, and Crosille & Villedieu 1992). One of the major advantages of dealing with the Boltzmann equation is that it reduces to a linear partial differential equation (PDE) in the Euler limit (as the collision term vanishes for the Maxwellian distribution). Designing an upwind scheme for this linear PDE is very much simpler than for the Euler equations which, as noted earlier, are nonlinear vector conservation equations. The principal subject matter of the present paper is to survey several Boltzmann schemes developed by the author and his coworkers and point out some promising future directions of research into the rapidly growing area of Boltzmann (also called kinetic) schemes.

2. Basic theory of Boltzmann schemes

Let us illustrate the basic idea with reference to 1-D unsteady Euler equations

$$(\partial U/\partial t)+(\partial G/\partial x)=0, \tag{1}$$

where U is the vector of conserved variables, G is the flux-vector and are given by

$$U=\begin{bmatrix}\rho\\ \rho u\\ \rho e\end{bmatrix}, \tag{2}$$

$$G=\begin{bmatrix}\rho u\\ p+\rho u^2\\ (\rho e+p)u\end{bmatrix}. \tag{3}$$

Here ρ = mass density, u = fluid velocity, p = pressure, e = total energy per unit mass $=p/[\rho(\gamma-1)]+(1/2)u^2$. Equation (1) can be obtained as the Ψ-moment of the 1-D Boltzmann equation (without the collision term)

$$(\partial F/\partial t)+v(\partial F/\partial x)=0, \tag{4}$$

where F is the Maxwellian velocity distribution given by

$$F=(\rho/I_0)(\beta/\pi)^{\frac{1}{2}}\exp[-\beta(v-u)^2-(I/I_0)] \tag{5}$$

$\beta=1/(2RT)$, R = gas constant per unit mass, v = molecular velocity, I = internal energy variable corresponding to nontranslational degrees of freedom, and

$$I_0=(3-\gamma)/[4(\gamma-1)\beta]. \tag{6}$$

The moment function vector is defined by

$$\Psi=[1,v,I+(v^2/2)]^T. \tag{7}$$

The Euler equations (1) can then be cast in the compact form

$$(\Psi,(\partial F/\partial t)+v(\partial F/\partial x))=0, \tag{8}$$

where the scalar product (Ψ,f) is defined by

$$(\Psi,f)=\int_0^{\infty}\mathrm{d}I\int_{-\infty}^{\infty}\mathrm{d}v\Psi f(v). \tag{9}$$

2.1 *KFLIC method*

Equation (8) is the basis of many kinetic schemes. One of the earliest schemes called kinetic-fluid-in-cell (KFLIC) method due to Deshpande & Raul (1982) exploits the above connection between the Euler equations and the Boltzmann equation. To obtain the state update formulae for the scheme let us consider 1-D interval $a\leqslant x\leqslant b$ which is assumed to be divided into cells. If a particle moves from $x\in C_i$ to $x'\in C_j$

during time interval Δt, then this particle will have molecular velocity $v = (x' - x)/\Delta t$. Hence the mass, momentum and energy transfer from cell C_i to C_j during Δt are given by

$$Ma(C_i \rightarrow C_j) = \int_{C_i} \mathrm{d}x \int_{C_j} \mathrm{d}x' [F(x, x')/\Delta t], \tag{10}$$

$$Mo(C_i \rightarrow C_j) = \int_{C_i} \mathrm{d}x \int_{C_j} \mathrm{d}x' [(x' - x)/\Delta t][F(x, x')/\Delta t], \tag{11}$$

$$En(C_i \rightarrow C_j) = \int_{C_i} \mathrm{d}x \int_{C_j} \mathrm{d}x' \{I_0 + [(x' - x)^2/2\Delta t^2]\}[F(x, x')/\Delta t], \tag{12}$$

where

$$F(x, x') = \rho(x)[\beta(x)/\pi]^{\frac{1}{2}} \exp\{-\beta(x)[((x' - x)/\Delta t) - u(x)]^2\}. \tag{13}$$

At the end of the transport of mass, momentum and energy from all cells C_i to the cell C_j, we have

$$Ma(C_j) = \sum_{\text{all } i} Ma(C_i \rightarrow C_j), \quad Mo(C_j) = \sum_{\text{all } i} Mo(C_i \rightarrow C_j),$$

$$En(C_j) = \sum_{\text{all } i} En(C_i \rightarrow C_j), \tag{14}$$

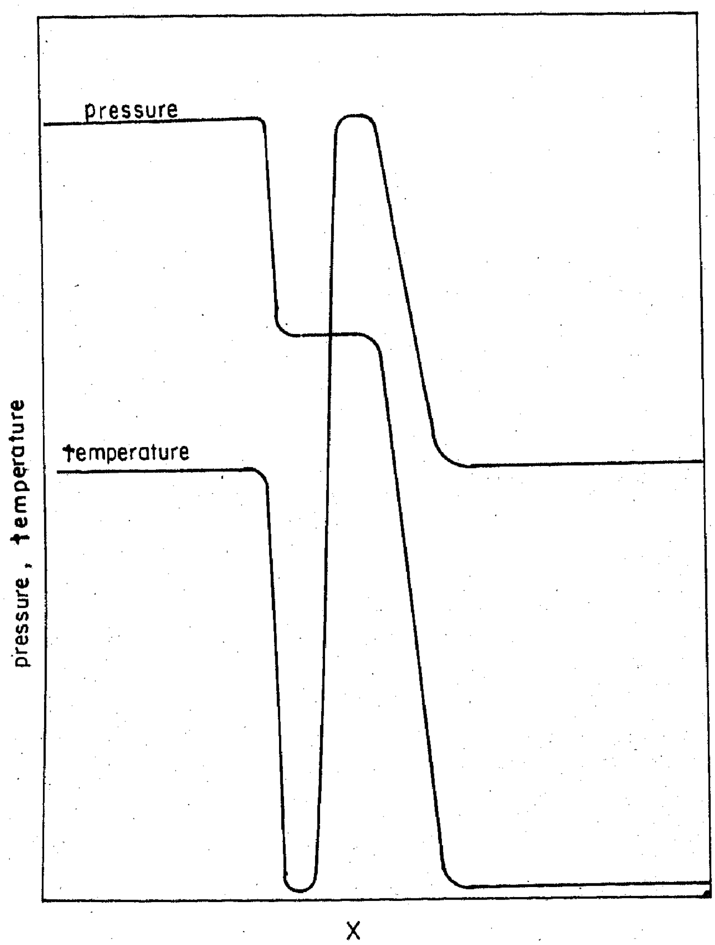

Figure 1. Application of KFLIC to 1-D shock propagation problem, no. of cells = 500 and $\Delta t = 10$.

which are the state update formulae for the method. Deshpande & Raul (1982) have used the KFLIC method for the 1-D shock propagation problem and the results are shown in figure 1. A large number of mesh points (500) were required for crisp shock. The KFLIC method is explicit, unconditionally stable, and first-order accurate in space and time. It can be regarded as a forerunner of Morton's characteristic Galerkin approach (Morton 1985). The method involves double integrals which have to be computed numerically and, hence, the method is computationally very expensive. Also, extension to multidimensions involves some problems in dealing with boundary conditions and keeping track of several possibilities as a particle moves from any cell to any other cell. Therefore this line of approach is not followed hereafter.

2.2 *Kinetic numerical method*

A faster version of the KFLIC method is the kinetic numerical method (KNM) which has the simple state update formula,

$$U_j^{n+1} = (\Psi, F^n(x_j - v\Delta t, v, I)), \tag{15}$$

where $F^n(x_j, v, I)$ is the local Maxwellian at the grid point x_j and time level n. Rietz (1981) was the first one who developed this KNM and applied it to the 1-D shock problem. Deshpande (1986a) has shown that the KNM satisfies the entropy condition, upwinding property and has TVD (total variation diminishing) property. For the purpose of proving that the entropy condition is satisfied, Deshpande (1986a) has used a slightly modified H function and flux-function H_v,

$$H = \iint \{F \ln F + [(5-3\gamma)/2(\gamma-1)] F \ln \beta\} \, dv \, dI,$$

$$H_v = \iint v\{F \ln F + [(5-3\gamma)/2(\gamma-1)] F \ln \beta\} \, dv \, dI, \tag{16}$$

and has further shown that these functions satisfy the entropy conservation

$$(\partial H/\partial t) + (\partial H_v/\partial x) = 0.$$

Developing higher order accurate versions of KNM is not straightforward. The difficulty arises due to the fact that the governing equations are (8) and not (4), hence it is not possible to construct higher order schemes for (8) by taking moments of higher order schemes of (4). We emphasize that $(\partial F/\partial t) + v(\partial F/\partial x) \neq 0$; in fact

$$\frac{\partial F}{\partial t} + v\frac{\partial F}{\partial x} = \left(\frac{\partial \rho}{\partial t} + v\frac{\partial \rho}{\partial x}\right)\frac{\partial F}{\partial \rho} + \left(\frac{\partial u}{\partial t} + v\frac{\partial u}{\partial x}\right)\frac{\partial F}{\partial u} + \left(\frac{\partial \beta}{\partial t} + v\frac{\partial \beta}{\partial x}\right)\frac{\partial F}{\partial \beta}. \tag{17}$$

The right-hand side of (17) is very characteristic of the Chapman–Enskog theory. Replacing the time derivatives of ρ, u, β above in terms of space derivatives using the Euler equations we get

$$(\partial F/\partial t) + v(\partial F/\partial x) = P_{CE}F, \tag{18}$$

where P_{CE} is a polynomial similar to the Chapman–Enskog polynomial and is given by*

*This polynomial is exactly the same as the polynomial that appears when Chapman–Enskog analysis is applied to the one-dimensional BGK model of the Boltzmann equation.

$$P_{CE} = (\partial u/\partial x)P_\tau + (\partial \beta/\partial x)P_q, \tag{19}$$

$$P_\tau = [(3\gamma - 5)/2] + (3-\gamma)[(v-u)^2/2RT] - [4(\gamma-1)^2/(3-\gamma)](I/2RT), \tag{20}$$

$$P_q = 5RT(v-u) - [4(\gamma-1)/(3-\gamma)]I(v-u) - (v-u)^3. \tag{21}$$

The polynomial P_{CE} has the interesting property

$$(\Psi, P_{CE}F) = 0. \tag{22}$$

We are now ready to construct the second-order accurate KNM of Deshpande (1986a, b). Start with

$$U^{n+1} = (\Psi, F^{n+1}) = (\Psi, F^n) + \Delta t[\Psi, (\partial F^n/\partial t)] + (\Delta t^2/2)[\Psi, (\partial^2 F^n/\partial t^2)] + \cdots.$$

Using (17) we obtain

$$U^{n+1} = (\Psi, F^n) - \Delta t[\Psi, v(\partial F^n/\partial x)] + \Delta t^2[\Psi, (\partial^2 F^n/\partial t^2)] + \cdots, \tag{23}$$

where we have used (18) and (22). For the second derivative $\partial^2 F/\partial t^2$ we have

$$(\partial^2 F/\partial t^2) = -v(\partial/\partial x)(\partial F/\partial t) + (\partial/\partial t)(P_{CE}F)$$
$$= v^2(\partial^2 F/\partial x^2) - v(\partial/\partial x)(P_{CE}F) + (\partial/\partial t)(P_{CE}F).$$

Substituting the above expression for the second derivative of F with respect to time in (23) and rearranging we get

$$U^{n+1} = (\Psi, F^n(x - v\Delta t)) - (\Delta t^2/2)[\Psi, v(\partial/\partial x)P_{CE}F] + O(\Delta t^3), \tag{24}$$

which shows that in addition to the $F^n(x - v\Delta t)$ term we have one more term containing the polynomial P_{CE}. Hence the Maxwellian distribution alone will not yield a second-order accurate KNM. Defining

$$f_{CE} = F[1 + (\Delta t/2)P_{CE}], \tag{25}$$

(24) can also be recast as

$$U^{n+1} = [\Psi, f^n_{CE}(x - v\Delta t)] + O(\Delta t^3). \tag{26}$$

When (25) is compared with the usual Chapman–Enskog distribution,

$$f_{CE} = F[1 - (\tau/p)P_\tau - (q\beta^{\frac{1}{2}}/p)P_q],$$

we observe that the distribution (25) is antidiffusive showing that such antidiffusive terms are necessary to achieve second-order accuracy. The first-order accurate KNM given by (15) is very diffusive as many first-order upwind methods are. The antidiffusive terms cancel this hefty amount of numerical diffusion to achieve second-order accuracy. Figure 2 shows the density and velocity plots for 1-D shock propagation problems solved by using the state update formula (26). Slope limiters have been used to suppress wiggles (Deshpande 1986a). It is observed that the method yields accurate results with high resolution.

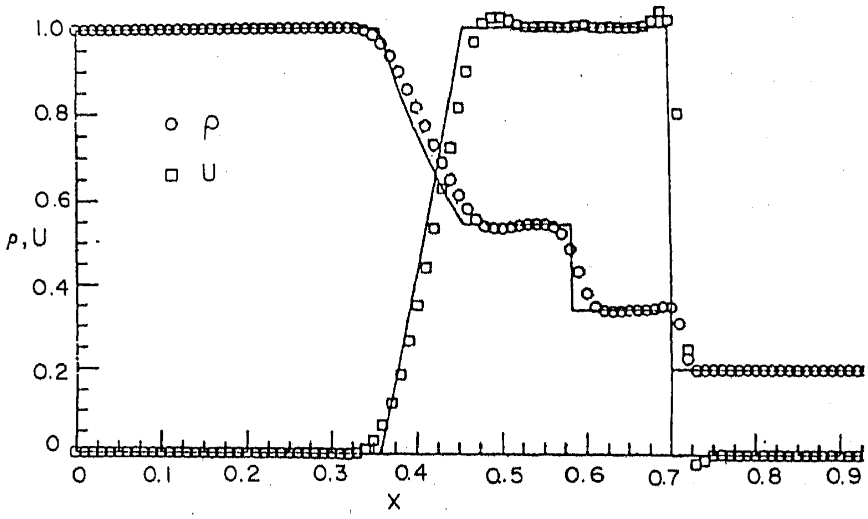

Figure 2. Computed and exact ρ and U profiles for shock tube problem with the antidiffusive Chapman–Enskog ansatz with TVD modification. $J = 101$, $t_A = 0{\cdot}00041$ s.

3. The kinetic flux vector splitting scheme

The KNM involves only one numerical integration with respect to the space variable and is therefore faster than the KFLIC method. It is tempting to enhance the speed further by modifying the KNM, and this can be accomplished by reducing its support. This brings us to the kinetic flux vector splitting (KFVS) scheme of Deshpande (1986b) and Mandal & Deshpande (1988). The KFVS method is obtained by splitting the Maxwellian into two parts corresponding to $v > 0$ and $v < 0$. The flux-vector G therefore splits as

$$G^+ = [\Psi, (v + |v|)/2F] \text{ and } G^- = [\Psi, (v - |v|)/2F]. \tag{27}$$

The split flux-vectors G^+ and G^- are integrals of $vF\Psi$ over positive and negative half spaces in velocity v. They can be evaluated in closed form in terms of error functions as

$$G^\pm = \begin{bmatrix} \rho u A^\pm \pm [\rho/2(\pi\beta)^{\frac{1}{2}}]B \\ (p + \rho u^2)A^\pm \pm [\rho u/2(\pi\beta)^{\frac{1}{2}}]B \\ (pu + \rho ue)A^\pm \pm [(p/2) + \rho e][B/2(\pi\beta)^{\frac{1}{2}}] \end{bmatrix}, \tag{28}$$

where

$$A^\pm = (1 \pm erfs)/2, \quad B = \exp[-s^2] \text{ and } s = \text{speed ratio} = u\beta^{\frac{1}{2}}.$$

In terms of the split fluxes the Euler equations become

$$(\partial U/\partial t) + (\partial G^+/\partial x) + (\partial G^-/\partial x) = 0. \tag{29}$$

Upwind differencing the split-flux terms in (29) we obtain the first order KFVS scheme

$$(\partial U/\partial t)_j^n + [(G_j^{+n} - G_{j-1}^{+n})/\Delta x] + [(G_{j+1}^{-n} - G_j^{-n}/\Delta x] = 0. \tag{30}$$

Substituting for U, G^+ and G^- in terms of F we get

$$(\partial/\partial t)(\Psi, F_j^n) + (1/\Delta x)[\Psi, (v+|v|)/2(F_j^n - F_{j-1}^n)] + (1/\Delta x)[\Psi, (v-|v|)/2(F_{j+1}^n - F_j^n)] = 0,$$

which is obviously the Ψ-moment of the Courant–Isaacson–Rees (CIR) differenced Boltzmann equation

$$(\partial F/\partial t)_j^n + [(v+|v|)/2][(F_j^n - F_{j-1}^n)/\Delta x] + [(v-|v|)/2][(F_{j+1}^n - F_j^n)/\Delta x] = 0. \tag{31}$$

Now an interesting question arises whether the KFVS scheme (30) which is obtained from (31) remains an upwind scheme after moments are taken. In order to demonstrate that the scheme (30) obtained by differencing (29) is an upwind scheme, it is necessary to transform (29) to a symmetric hyperbolic form. Deshpande (1986c) has shown that (29) can be transformed to

$$P(\partial q/\partial t) + B^+(\partial q/\partial x) + B^-(\partial q/\partial x) = 0, \tag{32}$$

where q is the transformed vector given by

$$q = [\ln \rho + [\ln \beta/(\gamma - 1)] - \beta u^2, 2\beta u, -2\beta]^T,$$

P is a positive symmetric matrix, and B^+, B^- are positive and negative symmetric matrices respectively. It then follows that $P^{-1}B^+$ and $P^{-1}B^-$ have real positive and real negative eigenvalues, respectively, thus justifying the backward differencing of $B^+(\partial q/\partial x)$ and forward differencing of $B^-(\partial q/\partial x)$. It has been found that the eigenvalues of $P^{-1}B^+$ and $P^{-1}B^-$ are smooth functions of the Mach number (Mandal 1989).

Mandal & Deshpande (1988) have shown that the above KFVS scheme can be made higher order accurate by following the analysis of Chakravarthy & Osher (1983). For this purpose we difference (29) as

$$(\partial U/\partial t)_j^n + [(G_{j+\frac{1}{2}}^n - G_{j-\frac{1}{2}}^n)/\Delta x] = 0. \tag{33}$$

The first-order KFVS given by (30) is obtained by choosing

$$G_{j+\frac{1}{2}} = [(G_j + G_{j+1})/2] + [DG_{j+\frac{1}{2}}^- - DG_{j+\frac{1}{2}}^+)/2], \tag{34}$$

where the flux differences $DG_{j+\frac{1}{2}}^{\pm}$ are defined by

$$DG_{j+\frac{1}{2}}^{\pm} = \{\Psi, [(v \pm |v|)/2](F_{j+1} - F_j)\} = (G_{j+1}^{\pm} - G_j^{\pm})/2. \tag{35}$$

Equations (33) and (34) express the KFVS scheme in a flux-difference splitting format implying that the KFVS scheme can also be looked upon as a flux-difference splitting scheme. Higher order schemes can now be obtained by modifying the formulae for $G_{j+\frac{1}{2}}$ as

$$G_{j+\frac{1}{2}} = \text{EFS} + (1/4)[(1+\phi)(DG_{j+\frac{1}{2}}^+ - DG_{j+\frac{1}{2}}^-) + (1-\phi)(DG_{j-\frac{1}{2}}^+ - DG_{j+\frac{3}{2}}^-)], \tag{36}$$

where the expression for the first order scheme (EFS) is the right-hand side of (34). The parameter ϕ takes on respectively the values -1 and $1/3$ for the second- and third-order upwind schemes. In order to suppress the spurious wiggles in the solution it is necessary to introduce the modified differences

$$\tilde{D}G^{\pm}_{j+\frac{1}{2}} = \mathrm{minmod}[DG^{\pm}_{j+\frac{1}{2}}, \tilde{R} \times DG^{\pm}_{j-\frac{1}{2}}] \tag{37}$$

$$\tilde{\tilde{D}}G^{\pm}_{j+\frac{1}{2}} = \mathrm{minmod}[DG^{\pm}_{j+\frac{1}{2}}, \tilde{R} \times DG^{\pm}_{j+\frac{3}{2}}] \tag{38}$$

where $\tilde{R}$ is a limiter with $0 \leqslant \tilde{R} \leqslant (3-\phi)/(1-\phi)$ and

$$\mathrm{minmod}[a,b] = [(\mathrm{sgn}(a) + \mathrm{sgn}(b))/2]\min[|a|,|b|], \tag{39}$$

$$\mathrm{sgn}(a) = +1, \text{ if } a > 0, \; -1 \text{ if } a < 0, \; 0{\cdot}0 \text{ if } a = 0{\cdot}0. \tag{40}$$

With these modified differences the formula (36) becomes

$$G_{j+\frac{1}{2}} = \mathrm{EFS} + (1/4)[(1+\phi)(\tilde{D}G^{+}_{j+\frac{1}{2}} - \tilde{\tilde{D}}G^{-}_{j+\frac{1}{2}}) + (1-\phi)(\tilde{\tilde{D}}G^{+}_{j-\frac{1}{2}} - \tilde{\tilde{D}}G^{-}_{j+\frac{3}{2}})]. \tag{41}$$

Figure 3 shows the computed density and fluid velocity profiles using the first-order, second-order and third-order KFVS schemes for which $G_{j+\frac{1}{2}}$ given by (34) and (41) are used. The accuracy of the results and the crispness of the shock are evident.

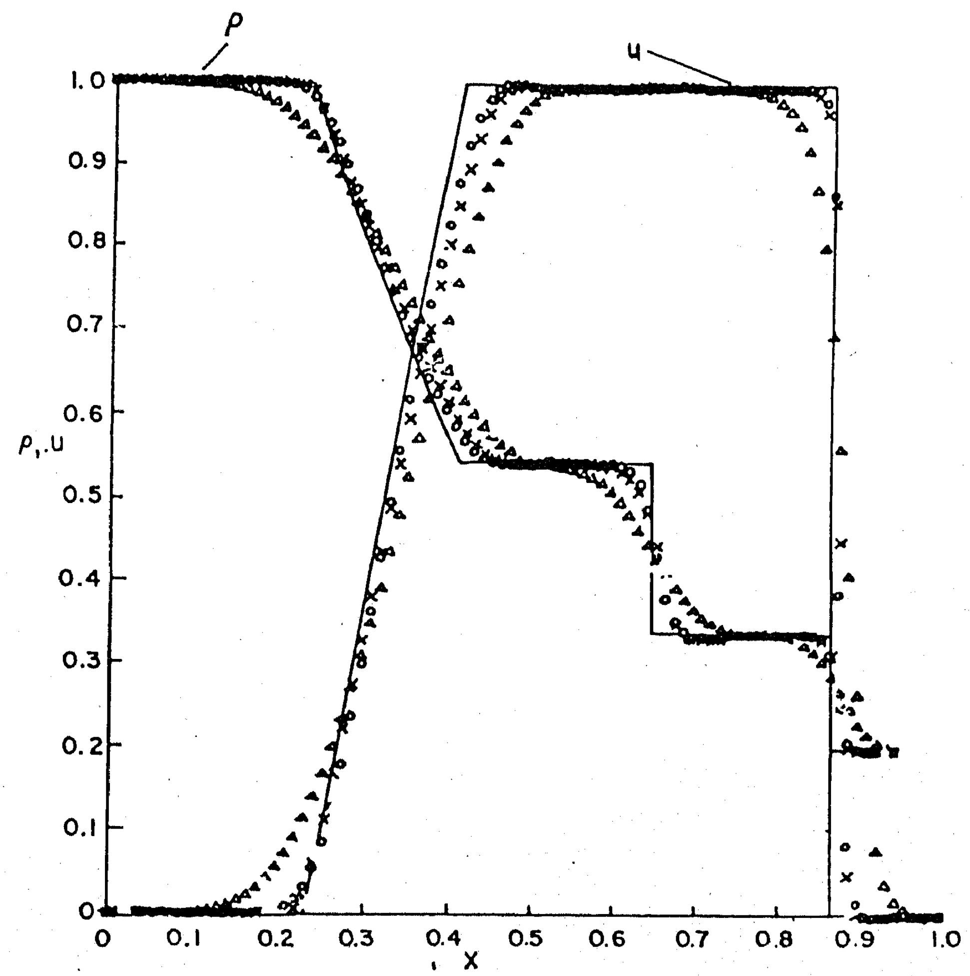

Figure 3. Computed ρ, u and exact (——) profiles for shock tube problems for KFVS. First order (△), second order (×) and third order (○).

4. KFVS applied to multidimensional flows

After having proved the capability of the KFVS method for a 1-D test case it is necessary to find out how it performs on 2-D and 3-D flows for low subsonic to hypersonic Mach numbers. Mandal (1989) has applied the high resolution finite volume KFVS method to the standard test cases of shock reflection and bump-in-a-channel problems. Figures 4 to 9 show the pressure contours and residue history for these problems. Mathur & Weatherill (1992) have applied the first order as well as high resolution KFVS schemes to a variety of 2-D problems with structured and unstructured meshes. They have used the cell-centred finite volume KFVS method. In order to use the high resolution KFVS method (which is a must in transonic regime) on a triangular mesh it is necessary to obtain the fluxes on the edges of a cell using extrapolation. Consider for example, a cell centre P of a triangular cell whose edges are shown hatched in I. The problem is to determine the flux on the edge AB in

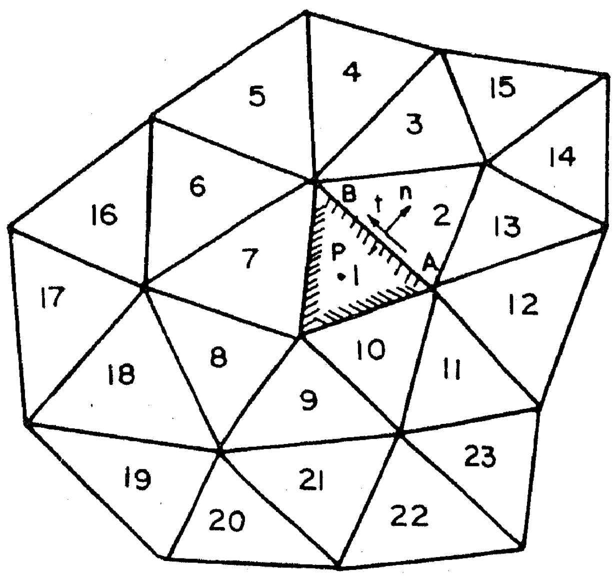

conformity with the upwinding principle. Let n be the outward normal to AB and t the tangent to the edge. Then applying the usual upwinding criterion we get

$$G_{AB} = G^{+}(u_{n1}, u_{t1}) + G^{-}(u_{n2}, u_{t2}). \tag{42}$$

Here we have suppressed the dependence of G^+ and G^- on density and temperature. In obtaining G_{AB} as above we have used only the data at cell centres 1 and 2. In order to obtain high resolution KFVS it is necessary to use the data at other neighbouring cell centres. Mathur & Weatherill (1992) consider the cell centres 13, 14, 15 and 3 and select that cell centre of this set which is closest to the straight line joining the centres 1 and 2. Assuming that this centre is 15, the flux G^{-}_{AB} is then obtained by extrapolation based on G^{-}_{2} and G^{-}_{15}. By using the same criterion G^{+}_{AB} can also be obtained. Obviously to suppress the wiggles minmod operators as explained before need to be used again. Figures 10 and 11 show typical results obtained by Mathur & Weatherill (1992) for the flow past an airfoil and flow through a ramp in a channel. They have made extensive comparisons between the results obtained by KFVS and Jameson's methods and concluded that the results obtained using the KFVS method generally compare favourably with those obtained using the Jameson scheme.

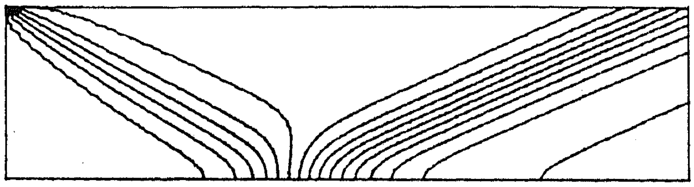

Figure 4. Pressure contours from 0·9 to 4·1 with an interval of 0·2 for shock reflection problem at supersonic Mach number ($M_\infty = 2{\cdot}9$, oblique shock angle = 29°) obtained using first-order time-marching finite difference KFVS scheme.

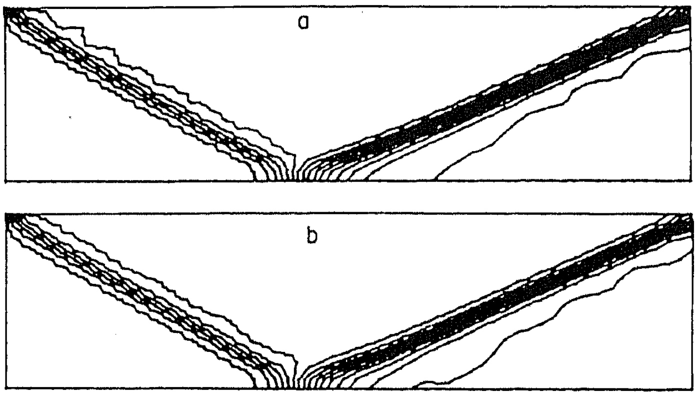

Figure 5. Pressure contours from 0·9 to 4·1 with an interval of 0·2 for shock reflection problem at supersonic Mach number ($M = 2{\cdot}9$, oblique shock angle = 29°) obtained using (**a**) second-order, and (**b**) third-order time-marching finite difference KFVS scheme.

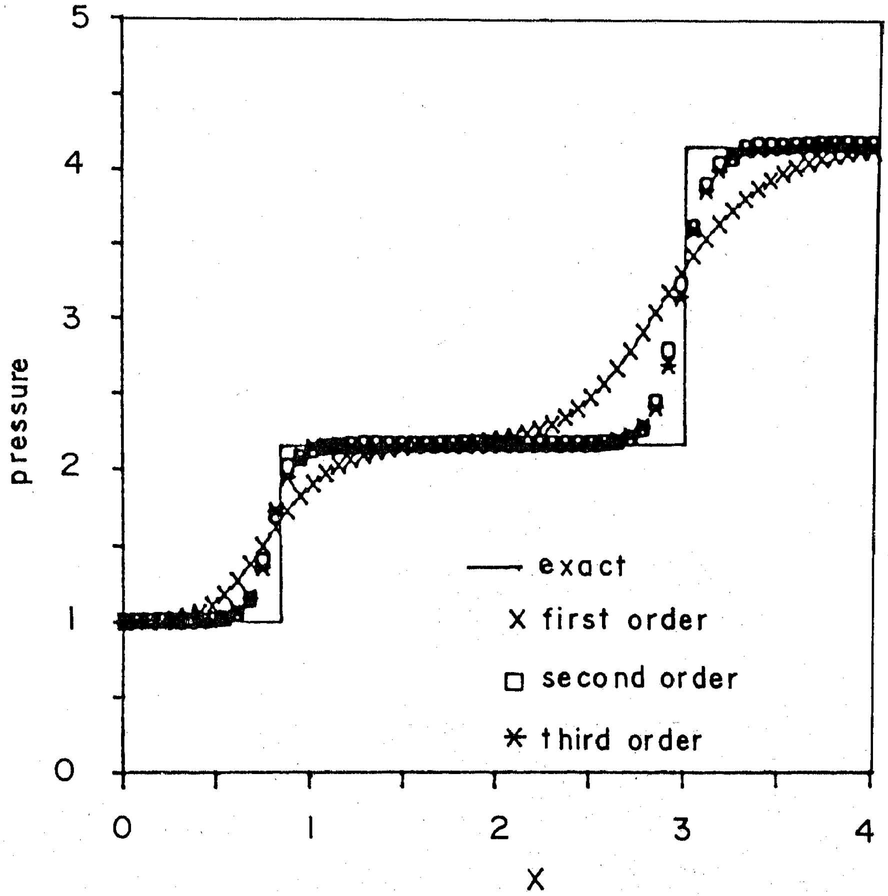

Figure 6. Pressure distribution at $y = 0{\cdot}5$ computed using first, second and third-order time-marching finite difference KFVS schemes.

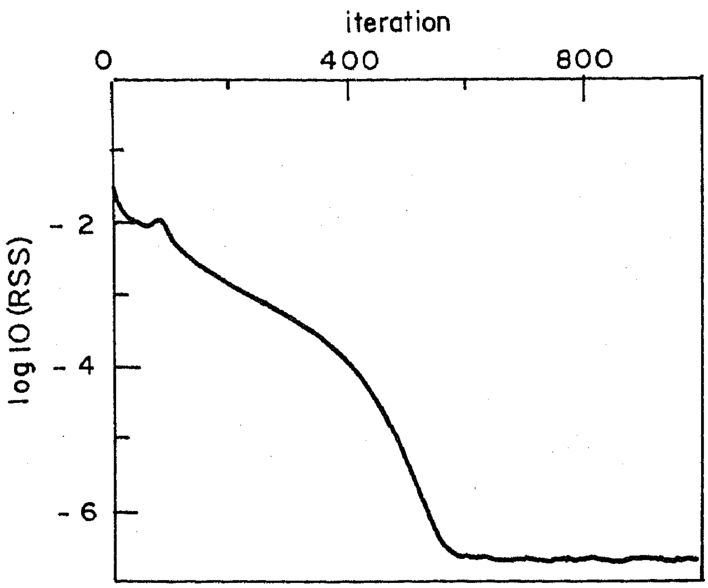

Figure 7. Convergence history for the shock reflection problem at supersonic Mach number using first-order time-marching finite difference KFVS scheme.

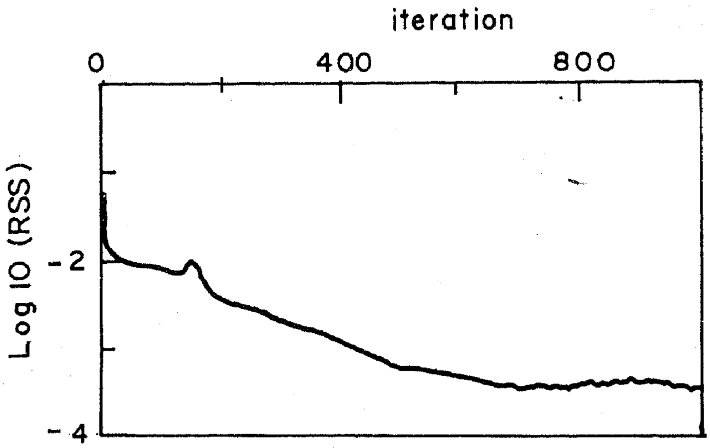

Figure 8. Convergence history for the shock reflection problem at supersonic Mach number using second-order time-marching finite difference KFVS scheme.

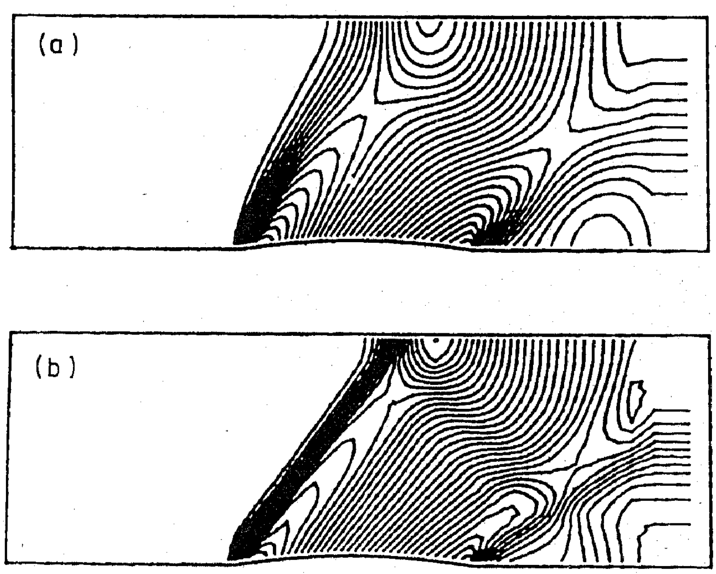

Figure 9. Pressure contours, from 0·65 to 1·45, with an interval of 0·025, for supersonic flow ($M_\infty = 1{\cdot}4$) over a 4% thick circular arc bump in a channel obtained using (**a**) first-order, and (**b**) high-resolution time-marching finite volume KFVS schemes.

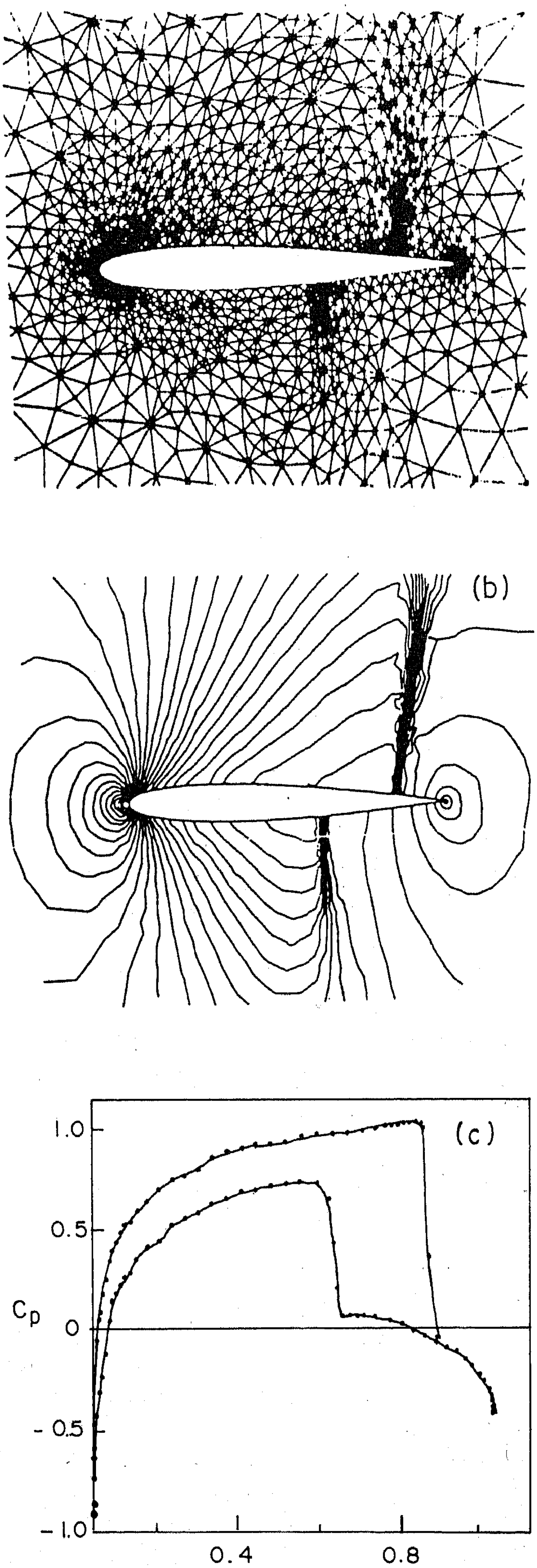

Figure 10. (**a**) Refined mesh, NACA 0012 airfoil. (**b**) Contours of pressure, refined mesh, KFVS. (**c**) C_p refined mesh, KFVS.

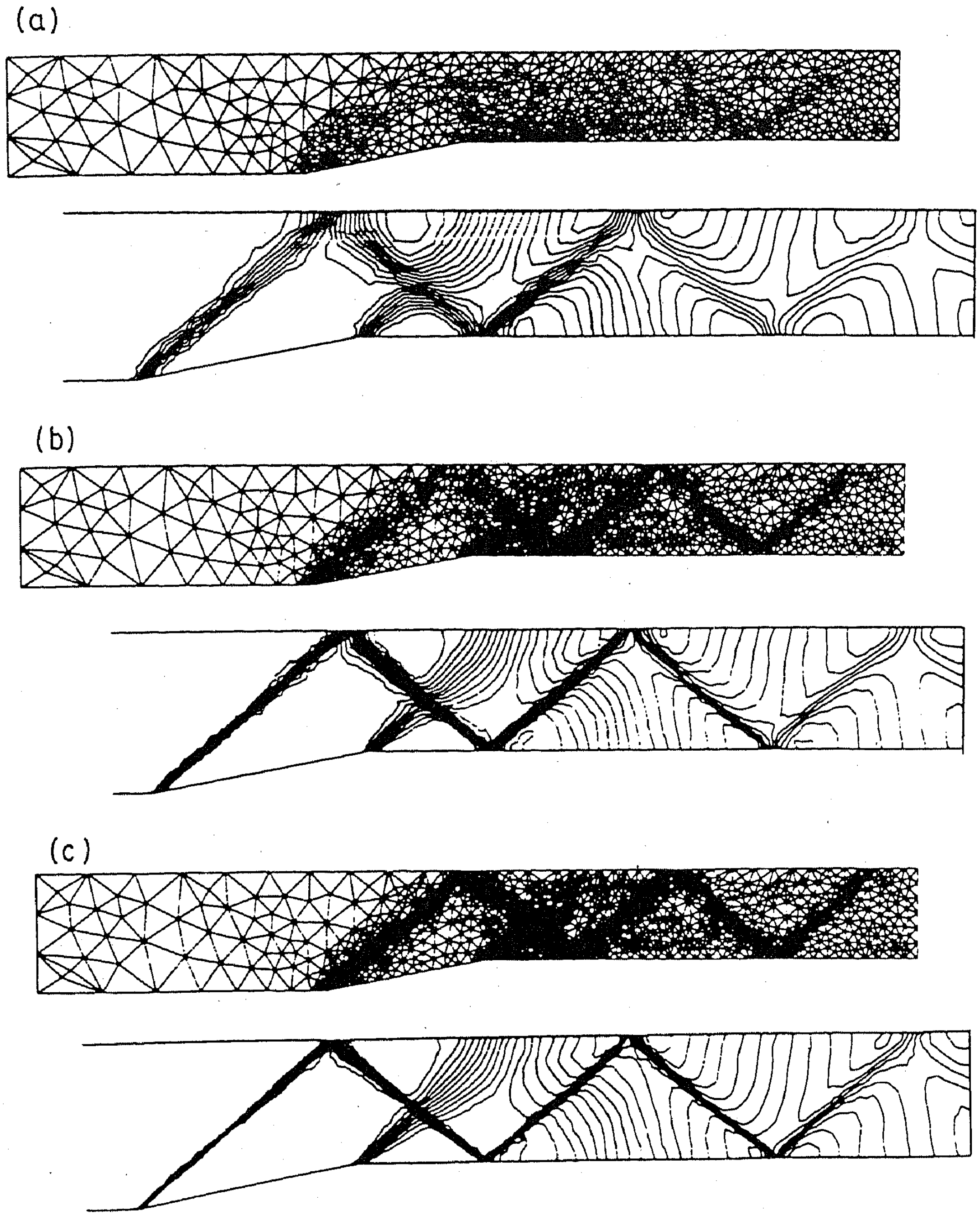

Figure 11. First (**a**), second (**b**), and third (**c**) refined meshes and contours of density.

Recently Deshpande *et al* (1992) have developed a 3-D time-marching Euler code (called BHEEMA) using the KFVS method for computing high speed flows around hypersonic re-entry configurations consisting of cone-cylinder-flares and control surfaces. This code uses finite volume method and operates on a hexahedral mesh generated by using stacked grids. Figures 12 and 13 show the pressure contours for axisymmetric configuration at $M = 4$ and $\alpha = 2°$, and a plot of the pressure coefficient for the re-entry configuration with wings at $M = 4$ and $\alpha = 0°$. Based on an elaborate comparison of the aerodynamic coefficients (C_A, C_N, C_M etc.) obtained from BHEEMA with the wind-tunnel results, they conclude that the time-marching 3-D Euler code

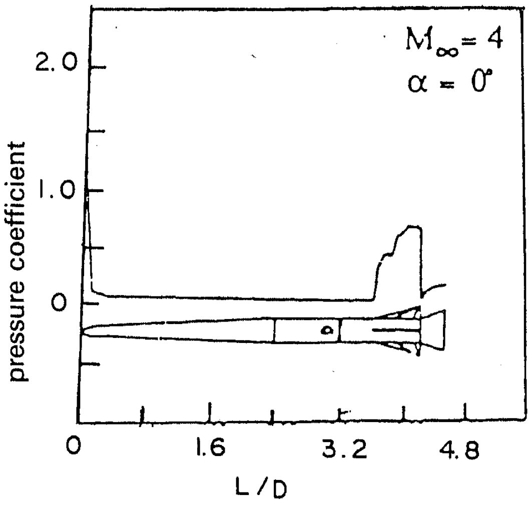

Figure 12. Pressure distribution along blunt cone-cylinder-flare (with lifting surfaces).

BHEEMA is a reliable design tool for predicting aerodynamic coefficients within 15%. Recently Deshpande & Dass (1992) have successfully used the convergence acceleration device called general minimum residual (GMRES) algorithm in combination with KFVS for obtaining faster convergence.

As a last example of the application of KFVS, mention may be made of the work of Theerthamalai & Deshpande (1992) who computed hypersonic reacting flow over a hemisphere using the KFVS method and an equilibrium chemistry model. For this purpose they considered 5 species (O, N, NO, O_2, N_2) and 3 reaction models

$$R_1:\ O_2 + M \rightleftharpoons 2O + M,$$

$$R_2:\ N_2 + M \rightleftharpoons 2N + M,$$

$$R_3:\ N_2 + O_2 \rightleftharpoons 2NO.$$

Here M stands for any one of the 5 species. For a specified γ the Euler equations were solved by BHEEMA for computing density, fluid velocity and temperature, everywhere in the flow field. Then the chemistry module was used to compute mass fractions, temperature and γ, everywhere in the flow field. The results of the computations reveal that the drag coefficient for Mach 10, 15, 20 was within 2% of that obtained by using

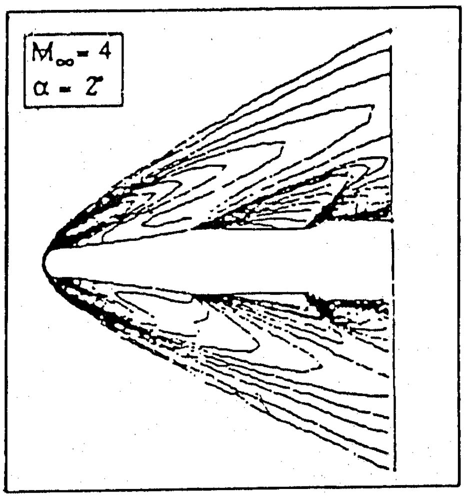

Figure 13. Iso-pressure contours for the configuration without lifting surfaces.

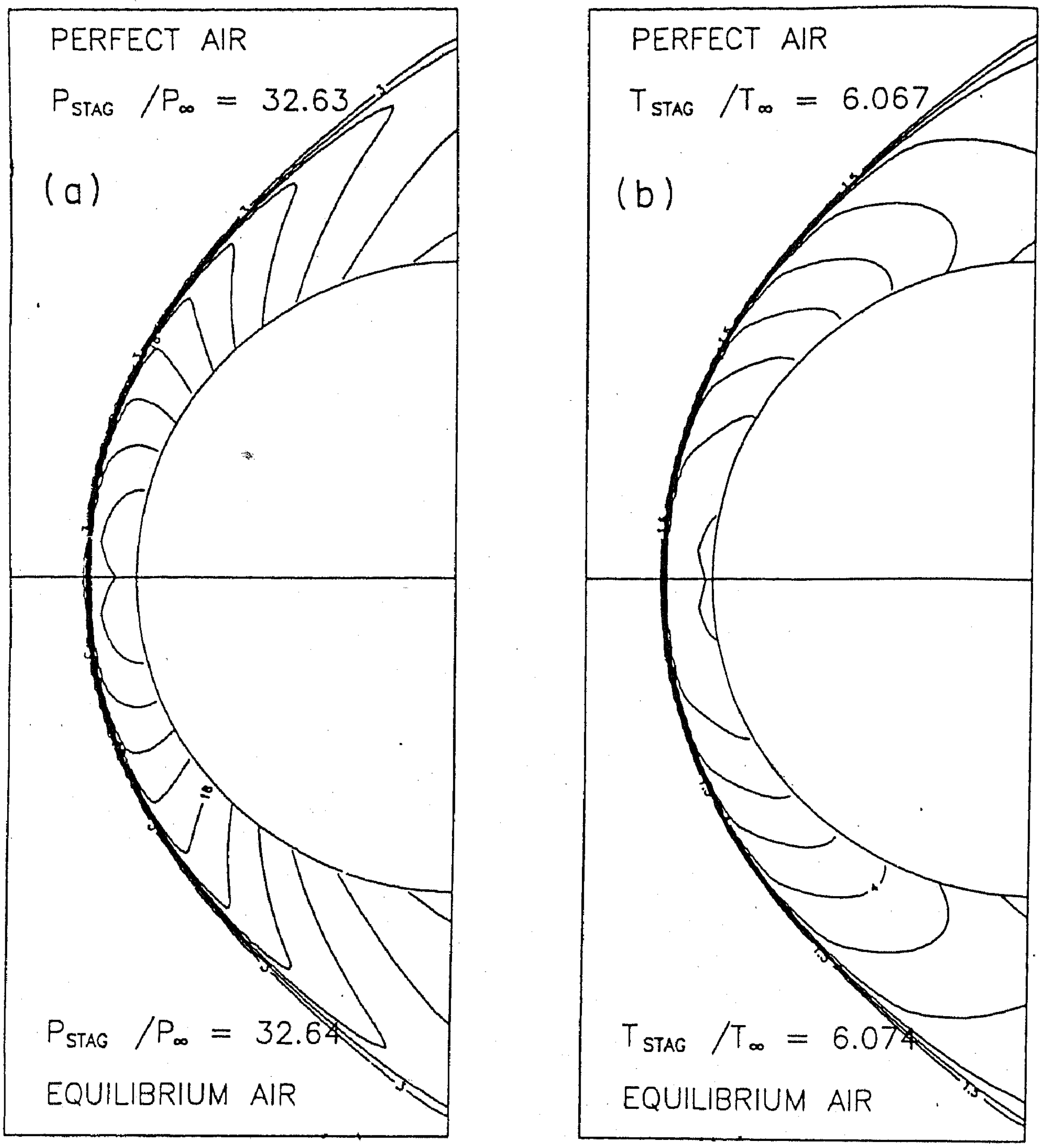

Figure 14. Pressure (**a**), and temperature (**b**) contours for reacting flow past a sphere (M = 5).

the nonreacting perfect gas model. However, the temperature differs substantially. Figures 14 and 15 show the temperature and pressure contours for $M_\infty = 5, 15$.

It is therefore reasonable to conclude that the KFVS method has travelled a long way since its modest beginning in 1982 and is now a fully tested and validated kinetic upwind method capable of computing inviscid compressible flows past any configuration.

5. Promising future directions

The search is continuously on for the elusive best method for obtaining numerical solutions of the Euler equations. The two guiding principles for developing new methods are that the method be less dissipative as compared to the existing ones

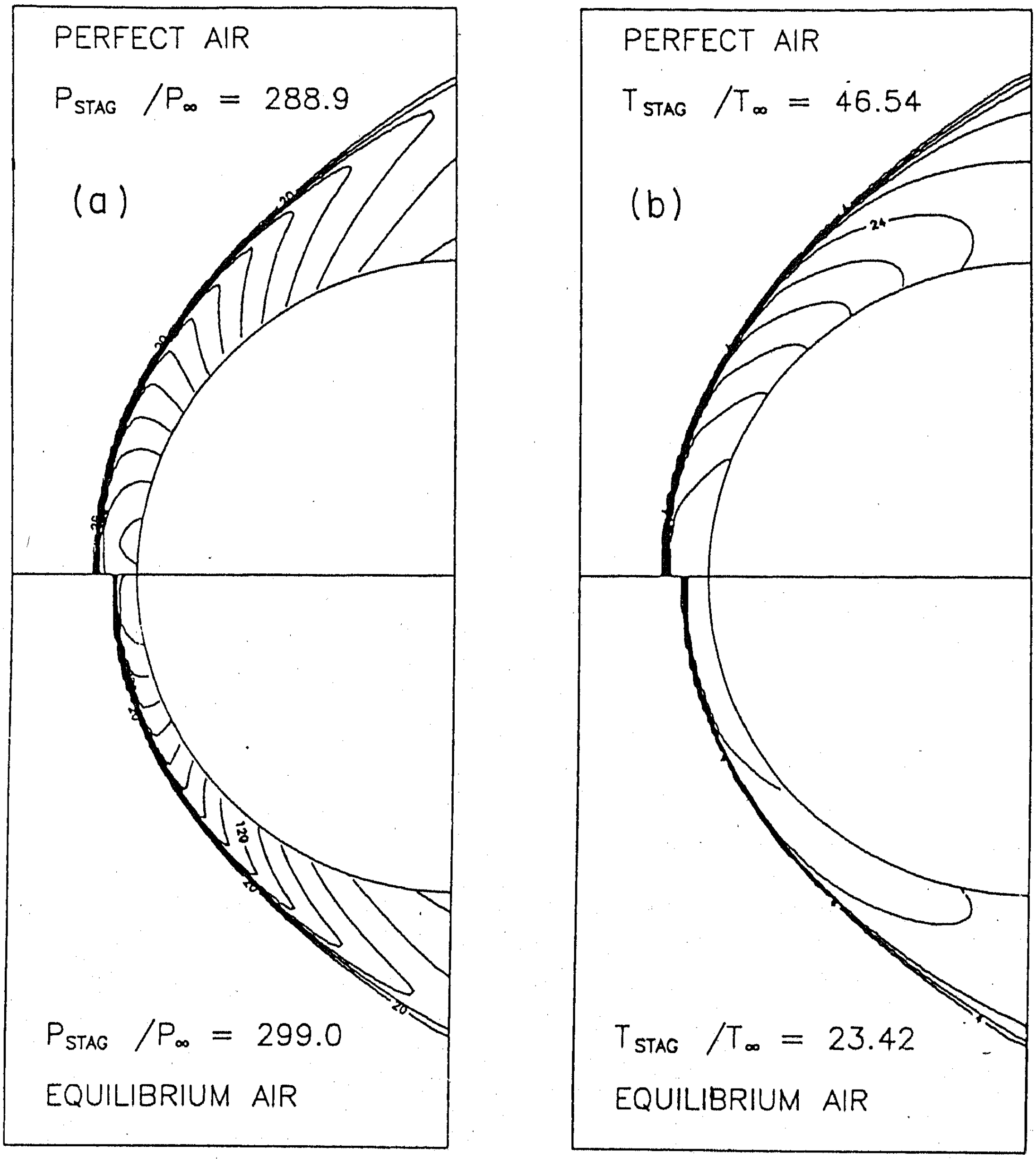

Figure 15. Pressure (**a**), and temperature (**b**) contours for reacting flow past a sphere (M = 15).

and further that it should mimic the physics of the flow as closely as possible. The development of upwind schemes is a consequence of following the second principle. We discuss briefly here four new ideas for developing upwind schemes exploiting the connection between the Boltzmann equation and the Euler equations.

5.1 *Use of exponential switch*

Considering the 1-D problem again for the sake of demonstrating the idea, we observe that KFVS is equivalent to assuming that the flux at the boundary B of a cell (see II) is given by

$$f_B = [(F_R + F_L)/2] - [(F_R - F_L)/2]\,\mathrm{sgn}(v). \tag{43}$$

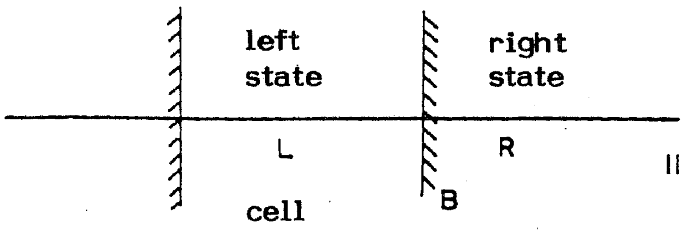

Here F_R and F_L are the Maxwellians corresponding to the right and left states, respectively, and sgn(v) is the usual sign function. We now replace the sign function by the exponential function giving

$$f_B = [(F_R + F_L)/2] - [(F_R - F_L)/2]\exp(-(\alpha|v|\Delta t)/\Delta x), \quad \text{for } v \geqslant 0,$$
$$f_B = [(F_R + F_L)/2] + [(F_R - F_L)/2]\exp(-(\alpha|v|\Delta t)/\Delta x), \quad \text{for } v \leqslant 0, \quad (44)$$

where α is a nonnegative real number. When the controlling parameter α is zero we get the standard KFVS scheme, and when α is infinity we obtain the central difference scheme which has zero diffusion. Thus by continuously varying α we can control the numerical diffusion in the scheme. Raghurama Rao & Deshpande (1991a) have applied the above scheme to the 1-D shock tube problem. The results are shown in figure 16 from which it is obvious that the above modification does reduce the diffusion in the scheme. Further investigation is essential to develop the idea even more.

5.2 *Kinetic splitting based on thermal velocity*

One of the criticisms that may be raised against the KFVS is that the method assumes the existence of the rest frame as the splitting of the flux requires the division of velocity space into two halves $v \geqslant 0$ and $v \leqslant 0$. As the rest frame is physically

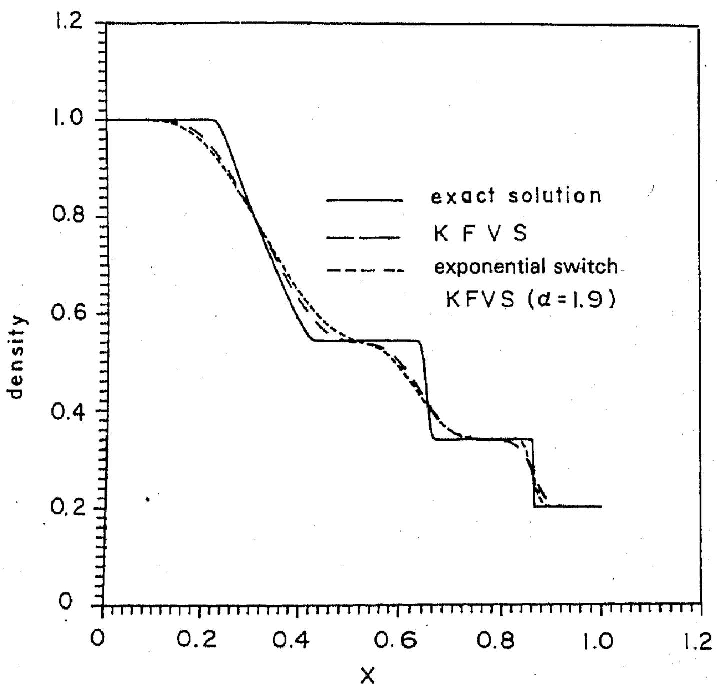

Figure 16. Results (KFVS) for 1-D shock tube problem.

meaningless it may be a good idea to do the splitting without assuming the existence of a rest frame. One possibility is to do the splitting based on the thermal (or what is also called peculiar) velocity. The thermal velocity **c** appears in the formulae for pressure, temperature and stress tensors of the kinetic theory of gases, and is thus physically more meaningful than the variable **v**. The motion of a molecule can be thought of as consisting of a random movement with velocity c superimposed on an orderly motion with velocity u. The random variable c is a Gaussian-distributed variable if we are dealing with inviscid gas dynamics. It may therefore be rewarding if a numerical scheme is constructed exploiting the above ideas. For the present we do splitting based on c. Towards this end we write the Boltzmann equation (without the collision term) in the form

$$(\partial F/\partial t) + u(\partial F/\partial x) + c(\partial F/\partial x) = 0. \tag{45}$$

Taking the moments we obtain

$$(\partial U/\partial t) + (\partial G^t/\partial x) + (\partial G^a/\partial x) = 0, \tag{46}$$

where

$$G^t = (u\Psi, F) = \begin{bmatrix} \rho u \\ \rho u^2 \\ \rho e u \end{bmatrix}, \quad \text{and } G^a = (c\Psi, F) = \begin{bmatrix} 0 \\ p \\ pu \end{bmatrix} \tag{47}$$

The eigenvalues of the flux Jacobian $(\partial G^t/\partial U)$ are all u, u, u showing that $(\partial G^t/\partial x)$ corresponds to the transport of fluid with velocity u. The eigenvalues of $(\partial G^a/\partial U)$ on the other hand are $0, \pm a[(\gamma - 1)/\gamma]^{1/2}$ where a is the local sonic velocity. The dynamics of the fluid can therefore be considered as being influenced partly by the particle motion (movement with velocity u) and partly by the wave motion (random movement or movement of waves with velocity $0, \pm a[(\gamma - 1)/\gamma]^{1/2}$). Loosely speaking the fluid motion can be considered partly particle-like and partly wave-like. Balakrishnan & Deshpande (1991, 1992) were the first ones who experimented with numerical schemes exploiting the wave–particle behaviour of fluid motion. Here we attack the problem from a different angle, namely, the construction of the Boltzmann scheme by treating the u and c terms differently. Following Raghurama Rao & Deshpande (1991a, 1992) we split G^a into G^{a+} and G^{a-}, defined by

$$G^{a+} = \{\Psi, [(c + |c|)/2]F\} \text{ and } G^{a-} = \{\Psi, [(c - |c|)/2]F\}, \tag{48}$$

which can be simplified as

$$G^{a\pm} = \begin{bmatrix} \pm \rho/2(\pi\beta)^{\frac{1}{2}} \\ (p/2) \pm [\rho u/2(\pi\beta)^{\frac{1}{2}}] \\ (pu/2) \pm [1/2(\pi\beta)^{\frac{1}{2}}][(p/2) + \rho e] \end{bmatrix} \tag{49}$$

Raghurama Rao & Deshpande (1991a, 1992) have solved the 1-D shock tube problem and 2-D shock reflection problem using the above upwind method (which they term the peculiar velocity based upwind (PVU) method). Figures 17 and 18 show the results obtained. The PVU method is found to be much less expensive compared to the KFVS method. The basic idea of treating uf_x and cf_x terms in a different fashion seems quite sound and definitely needs much more study and testing on a variety of multidimensional problems.

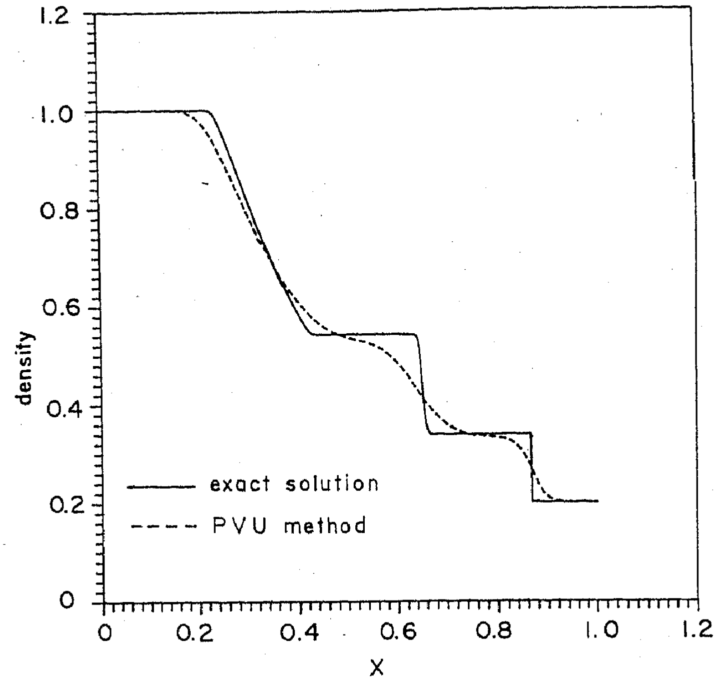

Figure 17. Results (PVU) for 1-D shock tube problem.

5.3 *Multidirectional Boltzmann schemes*

Many multidimensional upwind schemes advance the solution through a sequence of one-dimensional operators. The underlying physical model therefore involves wave propagation only along coordinate directions while the physical situation is that the

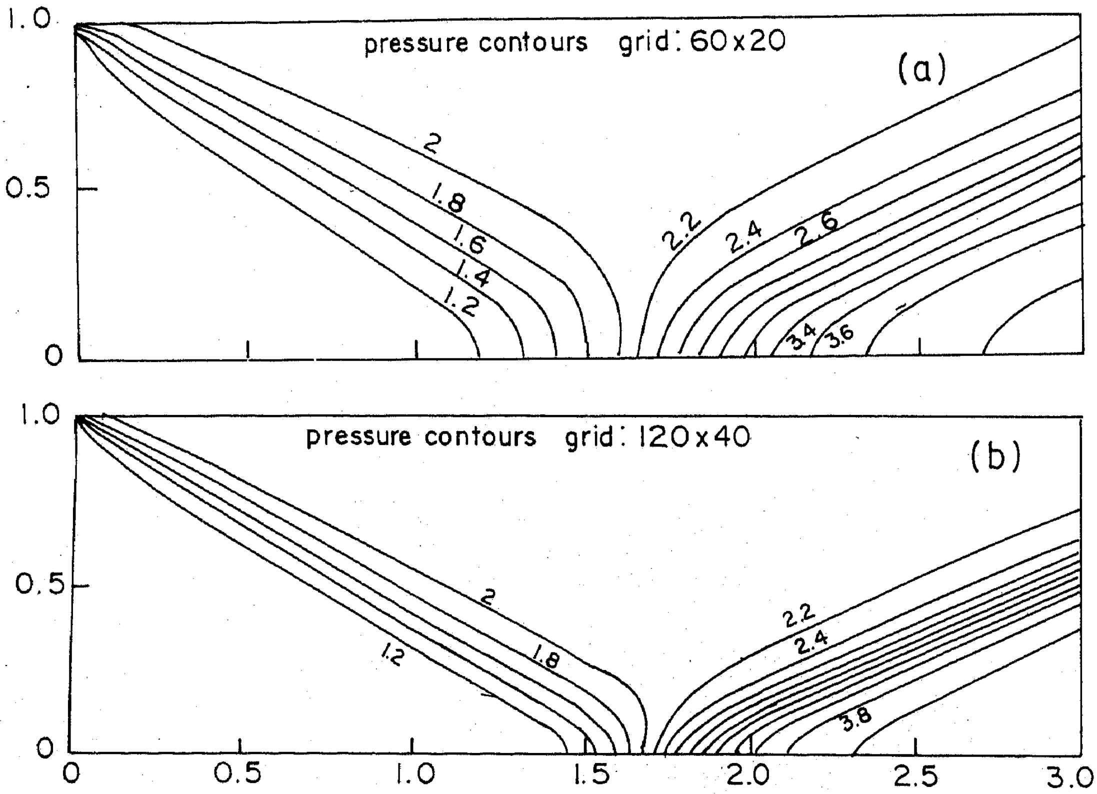

Figure 18. (a) & (b). Shock reflections with PVU method.

waves can propagate along all possible directions. Powell & Van Leer (1989) have observed that the inability to take the physics properly into account leads to a strong coupling between numerical schemes mentioned above and the grid on which they operate. Thus there is a need to design grid independent numerical schemes. Raghurama Rao & Deshpande (1991b) (see also Deshpande & Raghurama Rao 1992) have developed a genuinely multidimensional upwind Boltzmann scheme. Following the recent terminology this method can also be called the multidirectional upwind Boltzmann scheme.

Consider the Boltzmann equation without the collision term

$$(\partial f/\partial t) + \mathbf{v}\cdot(\partial f/\partial \mathbf{x}) = 0. \tag{50}$$

Considering a 2-D flow, the central problem in developing a multidirectional upwind scheme for the Euler equations (via the moment method strategy) is to develop a suitable discrete approximation to $v_1(\partial f/\partial x) + v_2(\partial f/\partial x)$ on the quadrilateral mesh, a portion of which is shown in III.

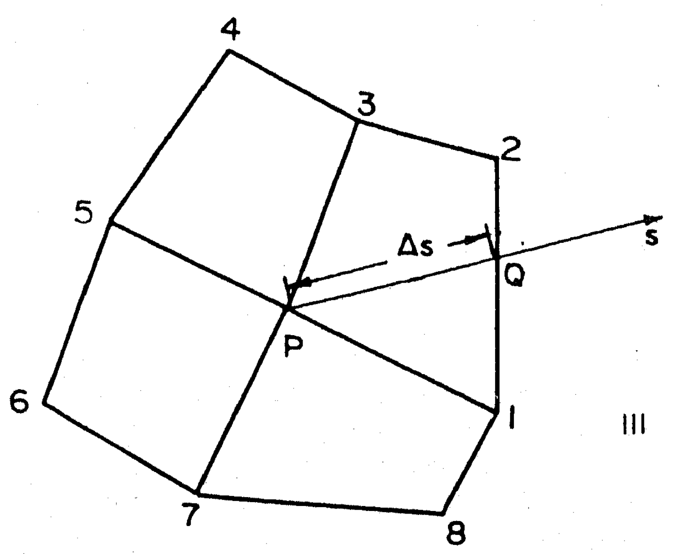

III

The mesh point P is surrounded by eight other mesh points. Particles arrive at P from all directions and *not* just along coordinate directions x and y since the molecular velocities v_1, v_2 vary from $-\infty$ to $+\infty$. The problem then boils down to obtaining a finite difference approximation to $\mathbf{v}\cdot grad\ f$ for each $\mathbf{v}$. Keeping in mind that $\mathbf{v}\cdot grad\ f = v(\partial f/\partial s)$, where s = coordinate along $\mathbf{v}$, we can obtain the first-order finite difference approximation as

$$v(\partial f/\partial s) = v[(f_P - f_Q)/\Delta s], \tag{51}$$

where Δs = distance between the points P and Q. We notice that on the right hand side of (51) the difference $f_P - f_Q$ appears instead of $f_Q - f_P$ because particles having velocity antiparallel to direction s send information to P. A slight rearrangement of (51) yields

$$v(\partial f/\partial s) = [v(\Delta n/\Delta s)][(f_P - f_Q)/\Delta n] = v_n[(f_P - f_Q)/\Delta n], \tag{52}$$

where Δn is the perpendicular distance of P from the segment 12. The next problem is to calculate f_Q from the data at the nodes $1, 2, \ldots, 8$. The position of the donor

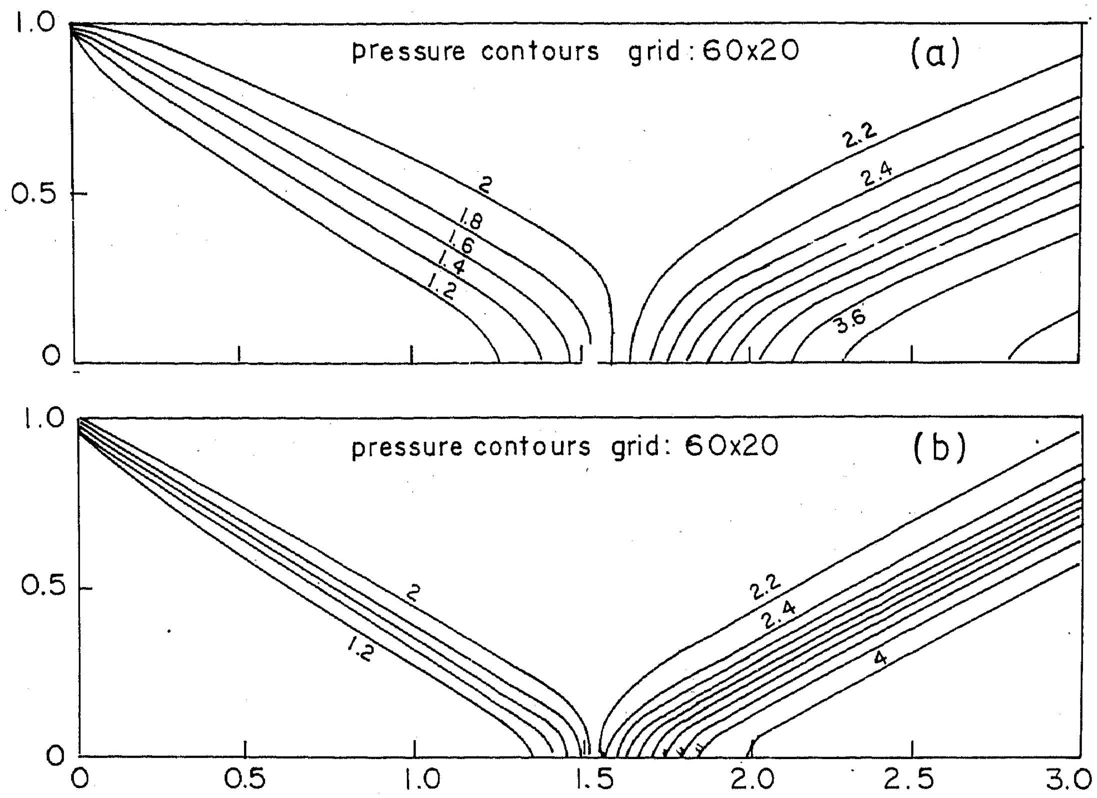

Figure 19. Shock reflections with KFVS (**a**) and GMBU (**b**) schemes.

point Q depends on the velocities (v_1, v_2) and could be anywhere on any of the eight segments $12, 23, \ldots, 81$. Consider the segment 12. Assuming linear variation between the nodes 1 and 2 the distribution function f_Q can be computed easily. Raghurama Rao & Deshpande (1991b) have given all the details involved in interpolation, obtaining appropriate limits of integration with respect to v_1, v_2. Of the two integrations they have been able to perform one, while the other one has to be performed numerically. Integrations with respect to velocities v_1, v_2 appear in the formulation when we pass from (51) to the Euler equations via the moment method strategy. As the resultant scheme takes into account all possible directions it is aptly called a multidirectional upwind Boltzmann scheme. They have applied this scheme to the standard shock reflection problem and the results are shown in figure 19 where the pressure contours from this scheme are compared with those from the usual KFVS scheme. It is obvious that the multidirectional scheme has much less smearing. Unfortunately, this scheme is very expensive and further research is necessary to improve it. Constructing a new multidirectional scheme using the thermal velocity is an attractive idea.

5.4 *Least squares weak upwind scheme*

Presently development of Euler solvers on unstructured meshes is mostly limited to finite element and finite volume based methods. The use of finite difference formulation on an unstructured grid is still a challenging task. Recently Deshpande *et al* (1988, 1989) have tackled this problem from a completely different point of view. At the heart of this formulation is the least squares discrete approximation to the derivatives f_x and f_y of any function f which in the present case is the Maxwellian velocity distribution

$$f = F = [\rho/2\pi RT]\exp\{-[(v_1 - u_1)^2/2RT] - [(v_1 - u_1)^2/2RT] - [I/I_0]\}. \tag{53}$$

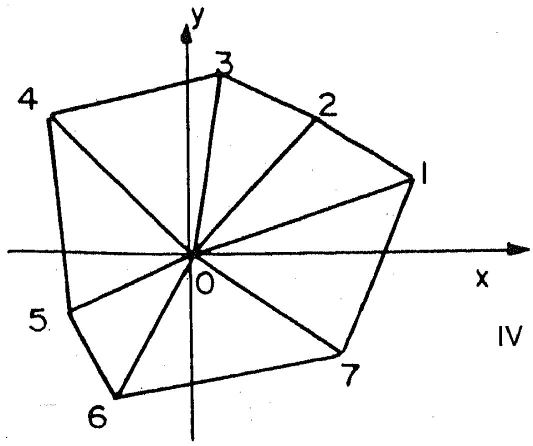

Let us consider a part of the triangular mesh shown in IV where the node O is surrounded by nodes 1, 2, 3, ... and let x_i, y_i be the coordinates of the node i. Introduce the notation

$$\Delta f_i = f_i - f_o, \quad \Delta x_i = x_i - x_o, \quad \Delta y_i = y_i - y_o.$$

The Taylor expansion gives

$$\Delta f_i = f_{xo}\Delta x_i + f_{yo}\Delta y_i, \quad i = 1, 2, \ldots, n. \tag{54}$$

Thus we have two unknowns f_{xo} and f_{yo} and n linear equations. By minimizing the square of the error

$$e = \sum_{i=1}^{n} (\Delta f_i - f_{xo}\Delta x_i - f_{yo}\Delta y_i)^2, \tag{55}$$

we get the least squares approximation

$$f_{xo} = \frac{\|\Delta y\|^2(\Delta x, \Delta f) - (\Delta x, \Delta y)(\Delta y, \Delta f)}{\|\Delta x\|^2\|\Delta y\|^2 - (\Delta x_1 \Delta y)^2}, \tag{56}$$

$$f_{yo} = \frac{\|\Delta y\|^2(\Delta y, \Delta f) - (\Delta x, \Delta y)(\Delta x, \Delta f)}{\|\Delta x\|^2\|\Delta y\|^2 - (\Delta x_1 \Delta y)^2}, \tag{57}$$

where

$$\|\Delta x\|^2 = \sum_{i=1}^{n} \Delta x_i^2, \quad \|\Delta y\|^2 = \sum_{i=1}^{n} \Delta y_i^2,$$

$$(\Delta x, \Delta f) = \sum_{i=1}^{n} \Delta x_i \Delta f_i, \quad (\Delta y, \Delta f) = \sum_{i=1}^{n} \Delta y_i \Delta f_i. \tag{58}$$

The formulae (56) and (57) are only first-order accurate. The second-order accurate approximations are obtained by replacing Δf_i in (56) and (57) by $\Delta \tilde{f}_i$ defined by

$$\Delta \tilde{f}_i = \Delta f_i - \tfrac{1}{2}\Delta x_i \Delta f_{xi} - \tfrac{1}{2}\Delta y_i \Delta f_{yi}, \quad \Delta f_{xi} = f_{xo} - f_{xi}, \quad \Delta f_{yi} = f_{yo} - f_{yi}. \tag{59}$$

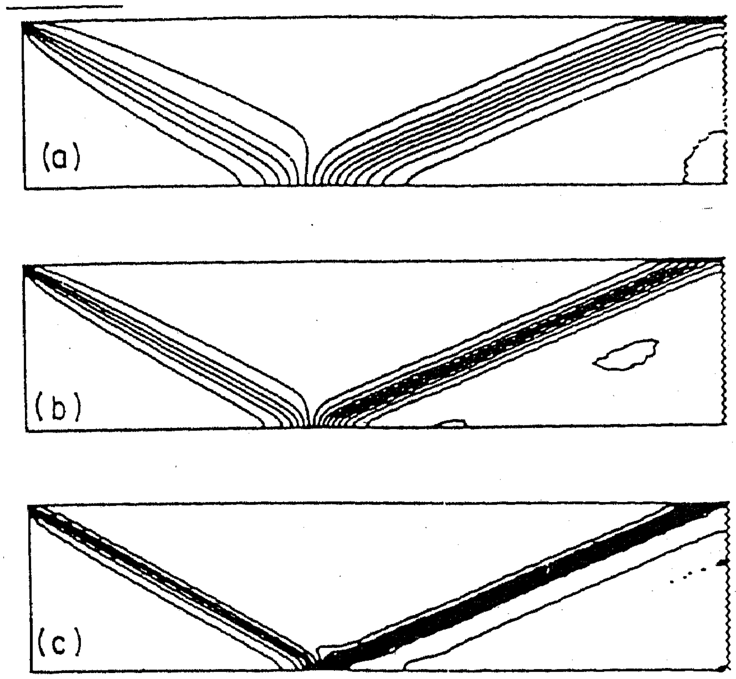

Figure 20. Pressure contours for shock reflection problem using least squares upwind method: first order without (**a**) and with (**b**) rotation; second order with rotation (**c**). (Contour levels 0·9 to 4·1 at intervals of 0·2.)

An upwind scheme for the solution of the 2-D Boltzmann equation

$$(\partial f/\partial t) + v_1(\partial f/\partial x) + v_2(\partial f/\partial y) = 0, \tag{60}$$

can now be constructed using the discrete approximation (56) and (57). For $v_1 > 0$ and for obtaining discrete upwind approximation to f_{xo} we take the stencil to the left of the y-axis, and for $v_1 < 0$ we take the stencil to its right. A similar approach can be used for obtaining the discrete upwind approximation to f_{yo}. We term this approach x–y splitting. It is important to note that we can locally rotate the coordinate system as (56) and (57) are valid for any arbitrary frame. It is possible to reduce the numerical diffusion in the scheme by locally rotating the x, y frame to x', y' such that the x'-axis is parallel to the local streamline and the y'-axis is normal to the streamline. We then do the upwinding for $f_{x'_o}$ along the x'-axis and take all the nodes around O for obtaining $f_{y'_o}$. Once (60) is upwind differenced the least squares weak upwind scheme for the Euler equations can be obtained by the moment method strategy. The capability of the method has been demonstrated on a 2-D shock reflection problem. The first-order scheme without rotation (x–y splitting in global frame) and with rotation (x–y splitting in local frame) and the second-order accurate scheme with rotation have been applied to this problem. The pressure contours are shown in figure 20. These plots show that the scheme with rotation even though of first order captures the shock crisply. The second-order scheme captures the shock even more crisply.

6. Concluding remarks

In this paper, an attempt has been made to survey the tremendous development that has taken place over the last ten years in kinetic schemes. We have concentrated on the work done in the field by the author and several of his coworkers; for lack of time and space, the contributions of other researchers have been only passingly referred to. The KFVS scheme and its other variants have made steady progress over the years from its modest beginning in the early eighties to a mature numerical method for computing 3-D flows. The richness of the *moment method strategy* has been amply demonstrated by considering many possible directions such as wave-particle splitting, least squares upwinding and multidirectional upwinding.

The work presented in this paper is based on the research work done by several graduate students at our laboratory and collaborators from research and development organizations within the country. The author is specially thankful to J C Mandal, S V Raghurama Rao, A K Ghosh, A K Dass, M Nagarathinam, S Sekar, R Krishnamurthy, P K Sinha and P S Kulkarni. Financial support obtained from the Indo-Soviet Integrated Long Term Programme of Coordination in Science and Technology and the Indo-French Centre for the Promotion of Advanced Research (IFCPAR)/Centre Franco-Indien pour la Promotion de la Recherche Advancé (CFIPRA) is gratefully acknowledged.

References

Balakrishnan N, Deshpande S M 1991 New upwind schemes with wave–particle splitting for inviscid compressible flows. 91 FM 12, Fluid Mechanics Report, Department of Aerospace Engineering, Indian Institute of Science, Bangalore

Balakrishnan N, Deshpande S M 1992 New upwind methods exploiting the wave–particle behaviour of fluid flow. Presented at IMACS *International Symposium on Mathematical Modelling and Scientific Computing* (Calcutta: Int. J. Services)

Chakravarthy S R, Osher S 1983 High resolution applications of the Osher upwind scheme for the Euler equations. AIAA Paper no. 83–1943

Croisille J P, Delorme P 1991 Kinetic symmetrizations and pressure laws for the Euler equations. Report 91-67, Universite de Paris – Sud, France

Croisille J P, Villedieu 1992 Kinetic flux splitting schemes for hypersonic flows. *Proceedings 13th International Conference on Numerical Methods in Fluid Dynamics* (Berlin: Springer-Verlag)

Deshpande S M 1986a A second order accurate kinetic theory based method for inviscid compressible flows. NASA Technical Paper 2613

Deshpande S M 1986b Kinetic theory based new upwind methods for inviscid compressible flows. AIAA Paper 86–0275

Deshpande S M 1986c On the Maxwellian distribution, symmetric form, and energy conservation for the Euler equations. NASA Technical Paper 2583

Deshpande S M, Dass A K 1992 GMRES acceleration of kinetic flux vector split Euler code. *Proceedings of the First European Conference on Computational Fluid Dynamics*, Brussels

Deshpande S M, Ghosh A K, Mandal J C 1989 Least squares weak upwind method for Euler equations. 89 FM 4, Fluid Mechanics Report, Department of Aerospace Engineering, Indian Institute of Science, Bangalore

Deshpande S M, Mandal J C, Ghosh A K 1988 Kinetic upwind method for inviscid gas dynamics. *Proceedings Commonwealth Advisory Aeronautical Research Council* (*CAARC*) *Specialists Meeting on CFD*, National Aeronautical Laboratory, Bangalore

Deshpande S M, Raghurama Rao S V 1992 A genuinely multi-dimensional upwind scheme based on kinetic theory for Euler equations. Presented at *IMACS International Symposium on Mathematical Modelling and Scientific Computing* (Calcutta: Int. J. Services)

Deshpande S M, Raul R 1982 Kinetic theory based fluid-in-cell method for Eulerian fluid dynamics. 82 FM 14, Fluid Mechanics Report, Department of Aerospace Engineering, Indian Institute of Science, Bangalore

Deshpande S M, Sekar S, Nagarathinam M, Krishnamurthy R, Sinha P K, Kulkarni P S 1992 A 3-dimensional upwind Euler solver using kinetic flux vector splitting method. *Proceedings 13th International Conference on Numerical Methods in Fluid Dynamics, Lecture notes in Physics.* (Berlin: Springer-Verlag) 414:

Elizarova T G, Chetverushkin B N 1985 Kinetic algorithms for calculating gas dynamic flows. *J. Comput. Math., Math. Phys.* 25: 1526–1533

Kaniel S 1988 A kinetic model for the compressible flow equations. *Indiana Univ. Math. J.* 37: 537–563

Mandal J C 1989 *Kinetic upwind method for inviscid compressible flows*, Ph D thesis, Department of Aerospace Engineering, Indian Institute of Science, Bangalore

Mandal J C, Deshpande S M 1988 Higher order accurate kinetic flux vector splitting method for Euler equations. *Proceedings of the Second International Conference on Nonlinear Hyperbolic Problems* (Aachen FRG) (Braunschweig: Vieweg) Also (1989) *Notes Numer. Fluid Mech* 24: 384–392

Mathur J S, Weatherill N P 1992 The simulation of inviscid compressible flows using an upwind kinetic method on unstructured grids. *Int. J. Numer. Methods Fluids* 15: 59–82

Morton K W 1985 Generalized Galerkin methods for nonlinear hyperbolic problems. *Comput. Methods Appl. Mech. Eng.* 52: 835–859

Perthame B 1990 Boltzmann type schemes for gas dynamics and the entropy property. *SIAM J. Numer. Anal.* 27: 1405–1421

Powell K G, Van Leer B 1989 A genuinely multidimensional upwind cell-vertex scheme for the Euler equations. AIAA Paper 89–0095

Pullin D I 1980 Direct simulation methods for compressible inviscid ideal gas flows. *J. Comput. Phys.* 34: 231–244

Raghurama Rao S V, Deshpande S M 1991a A class of efficient kinetic upwind schemes for compressible flows. 91 FM 11, Fluid Mechanics Report, Department of Aerospace Engineering, Indian Institute of Science, Bangalore

Raghurama Rao S V, Deshpande S M 1991b A genuinely multi dimensional upwind Boltzmann scheme for Euler equations. 91 FM 6, Fluid Mechanics Report, Department of Aerospace Engineering, Indian Institute of Science, Bangalore

Raghurama Rao S V, Deshpande S M 1992 New upwind methods for Euler equations using thermal velocity based flux splitting. Presented at *IMACS International Symposium on Mathematical Modelling and Scientific Computing* (Calcutta: Int. J. Services)

Rietz R D 1981 One-dimensional compressible gas dynamics calculations using the Boltzmann equation. *J. Comput. Phys.* 42: 108–123

Roe P L 1981 Approximate Riemann solvers, parameter vectors and difference schemes. *J. Comput. Phys.* 43: 357–372

Theerthamalai P, Deshpande S M 1992 Computation of hypersonic flows over a sphere using kinetic flux vector splitting scheme with equilibrium chemistry. *Proceedings 6th National Conference on Aerodynamics*, Aeronautical Development Establishment, Bangalore

Van Leer B 1982 Flux vector splitting for the Euler equations. *Lecture Notes in Physics* (Berlin: Springer Verlag) 170: 507–512